Multi-User Holographic Communications via Channel Operator Diagonalization

Claudio Iacovelli, Giovanni Iacovelli, *Member, IEEE,* and Symeon Chatzinotas, *Fellow, IEEE*

***Abstract*—This paper investigates a multi-user Holographic Multiple-Input Single-Output (MISO) system, where a continuous surface transmitter communicates with multiple dipole receivers. The channel is diagonalized by selecting an optimal basis for both the transmitter and receivers, with the complexity scaling linearly with the number of users. The spectral efficiency of the proposed eigen-based Holographic MISO (HMISO) system is analyzed and compared to that of a Fourier-based HMISO and a conventional fully-digital MISO system under additive white Gaussian noise. Results indicate that the proposed eigen-based HMISO outperforms both systems in terms of spectral efficiency.**

***Index Terms*—Holographic communications, electromagnetic channel, channel diagonalization, eigenvalue problem.**

I. Introduction

HOLOGRAPHIC Multiple-Input Multiple-Output (MIMO) [1] emerges as the natural evolution of classical MIMO technology. Indeed, holographic surfaces employ a massive, nearly-continuous, number of antenna elements confined in a finite area, to provide ultra-high precise wavefront shaping and spatial resolution. The latter is crucial in near-field regime where half-wavelength sampling is generally no longer sufficient to fully capture the spatial structure of the incoming field and hence fully exploit the extra spatial modes. To achieve this, the densely packed radiative elements modulate the amplitude of the signal generated through the Radio Frequency (RF) chains to convey information to user terminals [2]. Differently from MIMO, these surfaces can be equipped with a single RF chain per spatial mode, which collectively represent the system Degrees of Freedom (DoF). The generated electric current density at the transmitting surface produces an electric field which couples with the receiver antenna. The design of the source current density and receiver coupling basis functions are the electromagnetic-continuous equivalent of the classical discrete MIMO beamforming [2]. In this regard, the scientific literature already investigated different approaches to determine the shape of these bases [2]–[7].

The most common option is represented by Fourier modes [3]–[5], which indeed generate sharp beams which can be easily directed towards the desired target. However, in the HMIMO framework, the channel impulse response corresponds to the Green's function and its support extends to spatial infinity. Consequently, the integration of the Green's function in a bounded spatial domain of the receiver surface leads to crosstalk among spatial modes and hence interference among users.

For this reason, the optimal choice of basis is represented by the eigenfunction of the channel operator, which can be exploited as orthogonal streams, thus maximizing the channel capacity [6]. Similarly, when the electromagnetic field is modeled as a continuous random field, a spectral decomposition of the signal autocorrelation defines analogous orthogonal streams [8]. However, finding these optimal eigenfunctions analytically is generally intractable, especially in a continuous framework [9]. In fact, the space is typically discretized to transform the continuous eigenfunction problem into a Singular Value Decomposition (SVD) problem with a finite dimension. Exceptionally, by assuming (i) a parabolic approximation of the wavefront and (ii) a paraxial setup, Prolate Spheroidal Wave Functions (PSWFs) have been demonstrated to be optimal for linear arrays [6]. This result has been recently extended in [7] to the non-paraxial single-user scenario. However, the design of eigenfunctions, that can guarantee a good tradeoff between computational efficiency and communication performance, remains a challenge in a multi-user scenario.

Contribution: Starting from electromagnetic theory, a multi-user holographic Multiple-Input Single-Output (HMISO) channel model is formulated as a continuous-space eigenvalue problem between input and output modes, inherently delocalized across all terminals. To address the infinite-dimensional nature of the problem, we first model the receiver as dipoles, then we introduce an *ansatz* for the source modes which reduces the continuous eigenvalue problem to a discrete one. Its size scales linearly with the number of users, thus significantly lowering computational complexity.

A receiver basis set is then constructed by forming weighted sums of the discrete eigenvectors, such that each resulting function is spatially localized to a specific receiver. This construction enables the use of non-zero eigenvalues as interference-free orthogonal streams, achieving channel diagonalization.

Finally, the spectral efficiency of the proposed HMISO system is evaluated against a HMISO which employs Fourier modes and a conventional fully-digital MISO system under white Gaussian noise. The max-min optimization of the spectral efficiency demonstrates that the proposed eigen-based HMISO outperforms both Fourier-based HMISO and traditional MISO systems, for any Signal-to-Noise-Ratio (SNR) values or surface areas, while maintaining a constant number of RF chains and an overall lower computational complexity.

C. Iacovelli is an independent researcher (email: claudio.iacovelli@hotmail.it). G. Iacovelli and S. Chatzinotas are with the Signal Processing and Communications (SIGCOM) Research Group at Interdisciplinary Centre for Security, Reliability and Trust (SnT), University of Luxembourg, 1855 Luxembourg City, Luxembourg (emails: giovanni.iacovelli@uni.lu, symeon.chatzinotas@uni.lu).

II. Electromagnetic Communication Model

The considered time-invariant narrowband communication system, whose geometry is depicted in Fig. 1, involves a holographic surface $\mathcal{S}$ transmitting to a set of K single-antenna users through an infinite and homogeneous medium. The former is equipped with $N \geq K$ RF chains, which determines the number of DoF at the source.

A. Propagation

In a waveguide-based architectures [2], a current is generated starting from a baseband signal, which carries the information symbols $\mathbf{q} = [q_1, \dots, q_n, \dots, q_N]^{\mathsf{T}} \in \mathbb{C}^N$, measured in [A]. The latter is upconverted through RF chains to a high-frequency current which, by exciting a feed structure, injects an electromagnetic wave into a leaky waveguide. The reference wave is then conveyed to the radiative surface $\mathcal{S}$, which modulates its amplitude. The corresponding outgoing field is a current density living on $\mathcal{S}$ and can assume an arbitrary shape when the phase of the reference wave can be also modulated. Therefore, any current density $\mathbf{j}(\mathbf{r}) \in \mathbb{C}^3$, which we assume hereafter to be monochromatic with wavelength λ, is decomposed through an orthonormal basis $\mathbf{\Phi} = \{\boldsymbol{\phi}_1(\mathbf{r}), \dots, \boldsymbol{\phi}_n(\mathbf{r}), \dots, \boldsymbol{\phi}_N(\mathbf{r})\}$ with support in $\mathcal{S}$ as

$$\mathbf{j}(\mathbf{r}) = \sum_{n=1}^{N} q_n \boldsymbol{\phi}_n(\mathbf{r}), \tag{1}$$

$$\int_{\mathcal{S}} \boldsymbol{\phi}_n^{\mathsf{H}}(\mathbf{s}) \boldsymbol{\phi}_{n'}(\mathbf{s}) \mathrm{d}\mathbf{s} = \delta_{nn'}, \tag{2}$$

with $\mathbf{r} = [x, y, z]^{\mathsf{T}} \in \mathbb{R}^3$ being a generic point in the space, and $\delta_{nn'}$ the Kronecker delta. Then, if the basis is square-integrable in $\mathcal{S}$, one has

$$q_n = \int_{\mathcal{S}} \boldsymbol{\phi}_n^{\mathsf{H}}(\mathbf{s}) \mathbf{j}(\mathbf{s}) \mathrm{d}\mathbf{s}, \tag{3}$$

$$\int_{\mathcal{S}} \|\mathbf{j}(\mathbf{s})\|^2 \, \mathrm{d}\mathbf{s} \leq p. \tag{4}$$

With this, the current density is guaranteed to have a maximum power p, measured in [A/m^2] and [A^2], respectively. The current signal propagates in free space in the form of an electric field $\mathbf{e}(\mathbf{r}) \in \mathbb{C}^3$, measured in [V/m]:

$$\mathbf{e}(\mathbf{r}) = j\kappa Z_0 \int_{\mathcal{S}} \mathbf{G}(\mathbf{r}, \mathbf{s}) \mathbf{j}(\mathbf{s}) \mathrm{d}\mathbf{s}, \tag{5}$$

where $\kappa = \frac{2\pi}{\lambda}$ denotes the wavenumber, Z_0 represents the characteristic impedance in the vacuum, and

$$\mathbf{G}(\mathbf{r}, \mathbf{s}) = \left(\mathbf{I}_3 + \frac{\nabla_{\mathbf{r}} \nabla_{\mathbf{r}}^{\mathsf{T}}}{\kappa^2} \right) \frac{e^{j\kappa \|\mathbf{r}-\mathbf{s}\|}}{4\pi \|\mathbf{r}-\mathbf{s}\|} \in \mathbb{C}^{3\times 3} \tag{6}$$

is the dyadic Green's function.

B. Received signal

The signal received is the sum of the electric field $\mathbf{e}(\mathbf{r})$ generated by the source $\mathcal{S}$ and the electromagnetic noise $\mathbf{n}(\mathbf{r})$ produced by other sources. This signal is received by single-antenna users which are modeled as dipoles, as it is assumed that their distance from the source is much smaller than the antenna size. At these receivers, the impinging signal induces a current which is amplified, downconverted by the RF chains, which introduce a thermal noise, and processed to recover the transmitted data. In this work, the mathematical analysis of Section III will focus on the noiseless case. Then, in Section IV, we will analyze the impact of white Gaussian noise on the performance of the communication system. The electric field at the users is projected on a vector space defined by an orthogonal basis $\mathbf{\Psi} = \{\boldsymbol{\psi}_1(\mathbf{r}), \dots, \boldsymbol{\psi}_m(\mathbf{r}), \dots, \boldsymbol{\psi}_M(\mathbf{r})\}$, with support that is the collection $\mathcal{R} = \bigcup_k \mathcal{R}_k$ for $k = 1, \dots, K$ point-wise domains centered in $\mathbf{r}_k$, each one associated with a single receiver. As the electric field is decomposed by virtue of (1), the scalar form of the channel coupling coefficients per n-th input, m-th output mode and k-th receiver read

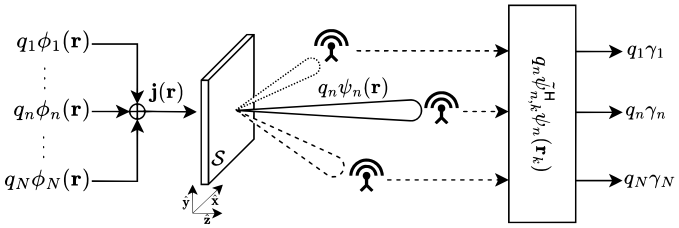

Fig. 1. Noiseless transmission scheme between an holographic surface $\mathcal{S}$ and a set of point-like receivers $\{\mathcal{R}_k\}$. The surface is centered in the $z = 0$ plane and the dipoles are placed at positions $\mathbf{r}_k$. The source basis functions $\boldsymbol{\phi}_n$ are chosen according to (15). The receiver-localized modes $\tilde{\boldsymbol{\psi}}_{n,k}$ are obtained by rotating the set of electric fields $\boldsymbol{\psi}_n$ as in (17).

$$h_{n,m,k} = j\kappa Z_0 \int_{\mathcal{R}_k} \int_{\mathcal{S}} \boldsymbol{\psi}_m^{\mathsf{H}}(\mathbf{r}) \mathbf{G}(\mathbf{r}, \mathbf{s}) \boldsymbol{\phi}_n(\mathbf{s}) \mathrm{d}\mathbf{s}\mathrm{d}\mathbf{r}, \tag{7}$$

where $h_{n,m,k}$ is a complex impendence measured in [Ω]. In the limit of a dipole, the characteristic function of each $\mathcal{R}_k$ is a Dirac delta, i.e., $\delta(\mathbf{r} - \mathbf{r}_k)$. Therefore, the integral in (7) simplifies to an evaluation for $\mathbf{r} = \mathbf{r}_k$. In the next Section, we will set the constant $j\kappa Z_0$ to unity for analytical convenience, and reintroduce it for the numerical analysis of Section IV.

III. Channel diagonalization

The main objective of this work is to derive the sets of orthogonal basis for both the source and the receivers which maximize the channel capacity by diagonalizing the channel, such that no cross-interference is observed among the users. This will be achieved with minimal signalling and without cooperation among users. To do so, we will first obtain an optimal set $\mathbf{\Phi}$ which induces a definition for $\mathbf{\Psi}$. Since this set is delocalized over all receivers, another set is defined through a rotation of $\mathbf{\Psi}$. This new set diagonalizes the corresponding channel with modes localized within single receivers.

Considering the whole receiving domain $\mathcal{R}$, the coupling coefficients between modes can be obtained by marginalizing over the users as

$$h_{n,m} = \sum_k \boldsymbol{\psi}_m^{\mathsf{H}}(\mathbf{r}_k) \int_{\mathcal{S}} \mathbf{G}(\mathbf{r}_k, \mathbf{s}) \boldsymbol{\phi}_n(\mathbf{s}) \mathrm{d}\mathbf{s}. \tag{8}$$

In order to maximize the transmitted power per mode [6], a good candidate for the receiver basis is

$$\boldsymbol{\psi}_n(\mathbf{r}) = \int_{\mathcal{S}} \mathbf{G}(\mathbf{r}, \mathbf{s}) \boldsymbol{\phi}_n(\mathbf{s}) \mathrm{d}\mathbf{s}, \tag{9}$$

which is proportional to free-space propagated electric field by the mode $\boldsymbol{\phi}_n$ in (5). This function is not normalized even if $\boldsymbol{\phi}_n$ is, and its substitution in (8) squares the dimension of the coupling coefficients, leading to:

$$h_{n,m} = \sum_k \left(\int_{\mathcal{S}} \boldsymbol{\phi}_m^{\mathsf{H}}(\mathbf{s}) \mathbf{G}^{\mathsf{H}}(\mathbf{r}_k, \mathbf{s}) \mathrm{d}\mathbf{s} \right) \left(\int_{\mathcal{S}} \mathbf{G}(\mathbf{r}_k, \mathbf{s}') \boldsymbol{\phi}_n(\mathbf{s}') \mathrm{d}\mathbf{s}' \right) = \int_{\mathcal{S}} \int_{\mathcal{S}} \boldsymbol{\phi}_m^{\mathsf{H}}(\mathbf{s}) \mathbf{K}(\mathbf{s}, \mathbf{s}') \boldsymbol{\phi}_n(\mathbf{s}') \mathrm{d}\mathbf{s}' \mathrm{d}\mathbf{s}, \tag{10}$$

where

$$\mathbf{K}(\mathbf{s}, \mathbf{s}') = \sum_k \mathbf{G}^{\mathsf{H}}(\mathbf{r}_k, \mathbf{s}) \mathbf{G}(\mathbf{r}_k, \mathbf{s}'), \tag{11}$$

represents the channel operator, which describes the interaction between source points $\mathbf{s}$ and $\mathbf{s}'$ through the propagation medium. It can verified that $\mathbf{K}(\mathbf{s}, \mathbf{s}')$ is a hermitian operator and hence admits a spectral decomposition. Then, the source basis functions $\boldsymbol{\phi}_n$ in (10) can be chosen to be the eigenfunctions of the channel operator, thus satisfying

$$|\gamma_n|^2 \boldsymbol{\phi}_n(\mathbf{s}) = \int_{\mathcal{S}} \mathbf{K}(\mathbf{s}, \mathbf{s}') \boldsymbol{\phi}_n(\mathbf{s}') \mathrm{d}\mathbf{s}', \tag{12}$$

with the eigenvalue equal to the power transmitted per mode. Now, the channel couplings are guaranteed to be diagonal when substituting (12) in (10):

$$h_{n,m} = |\gamma_n|^2 \int_{\mathcal{S}} \boldsymbol{\phi}_m^{\mathsf{H}}(\mathbf{s}) \boldsymbol{\phi}_n(\mathbf{s}) \mathrm{d}\mathbf{s} = |\gamma_n|^2 \delta_{nm}. \tag{13}$$

A. The source basis

Now, we seek a way to solve the eigenvalue equation (12) for $\boldsymbol{\phi}_n$. Taking advantage of the shape of the kernel $\mathbf{K}(\mathbf{s}, \mathbf{s}')$ in (11), the eigenvalue equation reads

$$|\gamma_n|^2 \boldsymbol{\phi}_n(\mathbf{s}) = \sum_k \mathbf{G}^{\mathsf{H}}(\mathbf{r}_k, \mathbf{s}) \int_{\mathcal{S}} \mathbf{G}(\mathbf{r}_k, \mathbf{s}') \boldsymbol{\phi}_n(\mathbf{s}') \mathrm{d}\mathbf{s}'. \tag{14}$$

This suggest the following *ansatz* for the basis functions

$$\boldsymbol{\phi}_n(\mathbf{s}) = \sum_k \mathbf{G}^{\mathsf{H}}(\mathbf{r}_k, \mathbf{s}) \boldsymbol{\chi}_{n,k}, \tag{15}$$

which is akin to a linear combination of electric fields produced by point-wise sources. Then, substituting (15) in (14):

$$\sum_k \mathbf{G}^{\mathsf{H}}(\mathbf{r}_k, \mathbf{s}) \Big(|\gamma_n|^2 \boldsymbol{\chi}_{n,k} - \sum_i \underbrace{\int_{\mathcal{S}} \mathrm{d}\mathbf{s}' \mathbf{G}(\mathbf{r}_k, \mathbf{s}') \mathbf{G}^{\mathsf{H}}(\mathbf{r}_i, \mathbf{s}')}_{\overline{\mathbf{K}}_{k,i}} \boldsymbol{\chi}_{n,i} \Big) = \mathbf{0}$$

$$\Rightarrow |\gamma_n|^2 \boldsymbol{\chi}_{n,k} = \sum_i \overline{\mathbf{K}}_{k,i} \boldsymbol{\chi}_{n,i} \;\Rightarrow\; |\gamma_n|^2 \boldsymbol{\chi}_n = \overline{\mathbf{K}} \boldsymbol{\chi}_n. \tag{16}$$

This new eigenvalue equation for the hermitian matrix $\overline{\mathbf{K}}$ is characterized by the same eigenvalues of $\mathbf{K}(\mathbf{s}, \mathbf{s}')$ and by the eigenvectors $\boldsymbol{\chi}_n = (\boldsymbol{\chi}_{n,k})_k^{\mathsf{T}}$. Note that the *ansatz* in (15), together with (16), implies the norm $\int_{\mathcal{S}} \|\boldsymbol{\phi}_n(\mathbf{s})\|^2 \mathrm{d}\mathbf{s} = |\gamma_n|^2$, so that the norm of $\boldsymbol{\psi}_n$ in (9) is $\sum_k \|\boldsymbol{\psi}_n(\mathbf{r}_k)\|^2 = |\gamma_n|^4$, assuming that $\boldsymbol{\chi}_n$ is normalized to unity.

B. The receiver basis

The electric field produced by the source modes obtained above is indeed the function $\boldsymbol{\psi}_n$ in (9) (except for $j\kappa Z_0$), which also gives the basis set the receivers use to process the signal. To recover the coupling coefficients $h_{n,m}$, it is needed to collect the signal from all receivers, which is not doable in case of different users. Consequently, one may think at the couplings $\tilde{h}_{n,k}$ between input mode n and a receiver k to be more significant. One first notices that when inserting (15) into (9) we have that $\boldsymbol{\psi}_n(\mathbf{r}_k) = \gamma_n \boldsymbol{\chi}_{n,k}$ based on the eigenvalue equation (16) with $\boldsymbol{\phi}_n$ normalized to unity. The channel $\tilde{h}_{n,k}$ can be obtained through a combiner $\mathbf{C}_{n,m,k} \in \mathbb{C}^{3\times 3}$ which realizes a weighted sum of the signal projected on all output modes fixed at the k-th receiver. It also rescales the channel to be measured as a complex impedance, when $j\kappa Z_0$ is reintroduced. This is equivalent to employ a new basis set

$$\tilde{\boldsymbol{\psi}}_{n,k} = \sum_m \mathbf{C}_{n,m,k} \boldsymbol{\psi}_m(\mathbf{r}_k) = \sum_m \gamma_m \mathbf{C}_{n,m,k} \boldsymbol{\chi}_{m,k}. \tag{17}$$

Given the new basis, the desired coupling coefficients read

$$\tilde{h}_{n,k} = \tilde{\boldsymbol{\psi}}_{n,k}^{\mathsf{H}} \boldsymbol{\psi}_n(\mathbf{r}_k) = \sum_m \boldsymbol{\psi}_m^{\mathsf{H}} \mathbf{C}_{n,m,k}^{\mathsf{H}} \boldsymbol{\psi}_n(\mathbf{r}_k) = \gamma_n \sum_m \gamma_m \boldsymbol{\chi}_{m,k}^{\mathsf{H}} \mathbf{C}_{n,m,k}^{\mathsf{H}} \boldsymbol{\chi}_{n,k}. \tag{18}$$

The expression above can be diagonalized with $\mathbf{C}_{n,m,k}^{\mathsf{H}} = \mathrm{diag}(\boldsymbol{\chi}_{m,\ell} \div \boldsymbol{\chi}_{n,k})/(3\gamma_m)$, with the division intended as pointwise in the spatial components. The index ℓ serves to associate a single receiver up to three input modes.

Finally, in order retrieve the channel $\tilde{h}_{n,k}$ proper dimensionality, one has to reintroduce the electric constants, so that $\tilde{h}_{n,k} = j\kappa Z_0 \gamma_n \delta_{\ell k}$. In summary, the channel operator modes are leveraged to convey information and obtained by diagonalizing the matrix $\overline{\mathbf{K}}_{k,i}$ in (16). The corresponding eigenvectors $\boldsymbol{\chi}_{n,k}$ are used to compute the source basis as in (15). Then, they are transmitted to receivers to calculate the optimal localized basis with equation (17).

C. Analysis

The channel operator diagonalization is initially stated as continuous eigenvalue equation in (12) for $\boldsymbol{\phi}_n(\mathbf{s})$ and then sent into a discrete one to be solved for $\boldsymbol{\chi}_n$. This formulation of the eigenvalue problem defines a number of modes $N = 3K$. Notably, in the far-field limit there are zero eigenvalues arising because of the dipole approximation. Indeed, in the same limit but in the case of a single receiver with spatial extension, the eigenfunctions of the channel correspond to PSWFs, which are characterized by non-zero eigenvalues. In the proposed setup, instead, the zero eigenvalue can be deduced in the case of a single receiver $K = 1$ from the first order asymptotic expansion of $\overline{\mathbf{K}}$. Its eigenvalues are equal to

$$\boldsymbol{\gamma}^2 = [0, 1, 1]|\mathcal{S}|/(16\pi^2 r^2), \tag{19}$$

where $r = r_i = r_k$ is the distance of the receiver and $|\mathcal{S}|$ is the area of the source. Specifically, the direction of the receiver is the eigenvector $(x, y, z)/r$ which corresponds to the zero mode, so one has a total of $2K$ non-zero modes for $\overline{\mathbf{K}}$. This

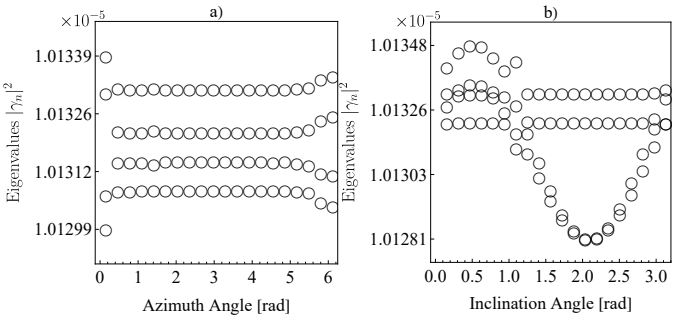

Fig. 2. Eigenvalues of the channel operator for $\varphi_1 = \pi/4$, $\theta_1 = \pi/3$, and $|\mathcal{S}| = 4$ m^2. a) is the scaling with respect to the azimuthal angle which separates the second receiver from the first for $\theta_2 = \pi/4$, $r_1 = r_2 = 50$ m. b) is the same with respect to the difference in the elevation angle, for $\varphi_2 = 3\pi/4$. Clearly, the discrepancy of these values from $\boldsymbol{\gamma}^2 = 1.01321\ 10^{-5}$ given by (19) is negligible.

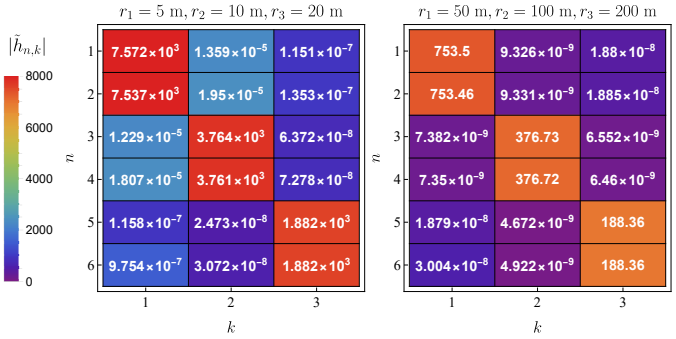

Fig. 3. Absolute value of the reconstructed channel $\tilde{h}_{n,k}$ for different radii set and $|\mathcal{S}| = 4$ m^2. The first two receivers are placed along the same angular directions as in Fig. 2a for $\varphi_2 = 3\pi/4$, while the third has $\varphi_3 = 5\pi/4$ and $\theta_3 = \pi/6$.

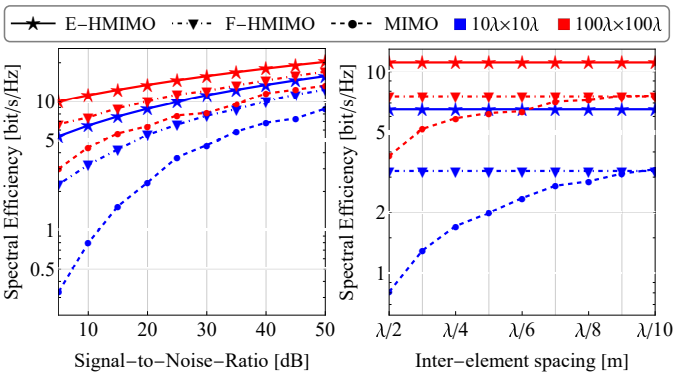

Fig. 4. Spectral efficiency of Eigen-HMISO (solid lines), Fourier-HMISO (dash-dotted), and MISO (dashed) for different surface lengths and same receiver configuration as in Fig. 3. Left: Spectral efficiency as a function of SNR, with a fixed inter-antenna spacing of $\lambda/2$ for MISO. Right: Scaling of MISO spectral efficiency with antenna spacing, using both HMISO systems as a reference, at a fixed SNR of 10 dB.

means that the projection of the source current along this direction does not transmit power, and hence information, to the receiver. Contrarily, the directions orthogonal to this transmit the same power, which determines the available polarizations of the electromagnetic wave. Although these eigenvalues are truly zero only for asymptotically large distances, they are, in practice, smaller then the others by orders of magnitude. Therefore, they will not be considered for transmission purposes hereafter. Note that the eigenvalue problem in (16) is agnostic with respect of the Green's function. For instance, a propagator which accounts for complex fading models or reflection from the ground can be adopted in place of (6). As a final remark, when $\|\mathbf{r}_k\| \gg \|\mathbf{r}_i\|$, one finds that $\left\|\overline{\mathbf{K}}_{k,i}\right\|_F \ll \left\|\overline{\mathbf{K}}_{k,k}\right\|_F \ll \left\|\overline{\mathbf{K}}_{i,i}\right\|_F$, that is, the product of two Green's functions pointed in different receivers averages to zero. This brings the matrix $\overline{\mathbf{K}}$ to acquire a block-diagonal form for those receivers. If this applies $\forall k = 1, \ldots, K$, the complexity of the diagonalization problem is reduced from $O((3K)^3)$ to $O(3^3 K)$, and could further reduced if a far-field, closed-form approximation of the channel matrix elements is empolyed in place of numerical integration [3], [5]. In contrast, computing the source eigenfunctions without the *ansatz* has a complexity of $O(N^6)$, with N being the discretization points in one spatial direction within $\mathcal{S}$. If $\overline{\mathbf{K}}$ is block-diagonal, an exact correspondence between eigenvalues and receiver is also established. Clearly, when more than one receiver is at the same distance from the source, different associations between eigenvalues and such receivers become available. The magnitude of the eigenvalues is determined by the path loss alone, and are numerically equal to (19). Instead, the eigenvectors $\boldsymbol{\chi}_n$ account for the presence of correlation.

IV. Numerical Results

In this Section, the above derivations are employed to obtain numerical results regarding the investigated HMISO communication system. The receivers are positioned, using spherical coordinates, in $\mathbf{r}_k = r_k[\sin\theta_k \cos\varphi_k, \sin\theta_k \sin\varphi_k, \cos\theta_k]$. The first considered scenario involves $K = 2$ receivers and a holographic surface placed in the origin, which transmits signals to the users with $\lambda = 0.01$ m. Fig. 2 shows the eigenvalues of the channel operator $\overline{\mathbf{K}}$ computed via (16) as functions of the azimuth and elevation angles difference between receivers. As it can be seen, the spherical angle variations produce only little changes in the eigenvalues, so their magnitude is mostly determined by (19), i.e., proportional to the inverse of the radius squared. Fig. 3 illustrates the reconstructed channel $\tilde{h}_{n,k}$ in (18) for $K = 3$ receivers and for different distances. Here, the input-output relation is realized with $\ell = (n + \mathrm{mod}(n, 2))/2$ because it establishes the correct correspondence if the input modes are arranged in descending order of the eigenvalues and the receivers in increasing order of the distance. Clearly, the proposed bases are able to diagonalize the channel as $\delta_{\ell k}$ in both cases. Fig. 4 compares the spectral efficiency of the proposed HMISO system against a classical, fully-digital MISO system and a HMISO which employs all available Fourier modes for the source basis. For the proposed HMISO system, one eigenvalue per receiver is selected as symbol to be transmitted and receiver through the eigenmodes (15) and (17), respectively. The fully-digital MISO channel coupling coefficients have been computed by assuming uniform current distributions for both the source and receiving antennas. Specifically, the MISO planar array is cross-polarized and each transmit antenna source mode is modeled as $\boldsymbol{\phi}_0 = [1, 1, 0]^{\mathsf{T}}/\sqrt{2}$ around the

antenna centers $\mathbf{s}_n$ through a spatial extension of $(\lambda/10)^2$. The receivers are described with an isotropic polarization $\boldsymbol{\psi}_0 = [1,1,1]^\mathsf{T}/\sqrt{3}$ and modeled as dipoles through a delta-like extension centered at $\mathbf{r}_k$. Then, the MISO couplings are computed with (8) for $\boldsymbol{\phi}_n = \boldsymbol{\phi}_0$ and $\boldsymbol{\psi}_m^\mathsf{H} = \boldsymbol{\psi}_0^\mathsf{H}$. As the Green's function slowly varies within the single antenna, the couplings read $h_{n,k} \simeq j\lambda^2\kappa Z_0 \sum_i^3 \sum_j^2 G_{ij}/(100\sqrt{6})$, with $G_{ij} = G_{ij}(\mathbf{r}_k, \mathbf{s}_n)$ being the (i,j)-th entry of the Green's function (6). Also, the antenna elements at the source are equally spaced to patch the size of the holographic surface In this study, the effects of mutual couplings are neglected. Indeed, while they could enhance MISO's spectral efficiency if properly leveraged, their presence otherwise degrades performance beyond $\lambda/2$ [10]. Finally, the couplings for the HMISO source which employs Fourier modes are also computed with (8) for $\boldsymbol{\phi}_n = (\mathbf{x}+\mathbf{y})e^{i\mathbf{k}_n\mathbf{x}}/(\sqrt{2}a)$ and $\boldsymbol{\psi}_m^\mathsf{H} = \boldsymbol{\psi}_0^\mathsf{H}$. In the former, $\mathbf{x}$ and $\mathbf{y}$ define the directions in the plane, a is the surface length, and $\mathbf{k}_n = 2\pi[n_x, n_y]^\mathsf{T}/a$ is the spatial wavenumber. Fig. 4 compares the minimum spectral efficiency (SE) for the HMISO and MISO systems that can be achieved through a max-min rate optimization. The proposed eigen-based HMISO SE presents no interference due to the nature of the proposed framework, so it can be expressed as:

$$\mathrm{SE}_k = \log_2(1 + |\tilde{h}_{2k-1,k}|^2 p_k/\rho), \tag{20}$$

where ρ denotes the inverse SNR, p_k are the power allocation coefficients satisfying $\sum_k p_k \leq 1$, and the indexing defines the eigenvalue selection, given that $\tilde{h}_{n,k} \propto \delta_{\ell,k}$. The corresponding MISO and Fourier-HMISO SEs read

$$\mathrm{SE}_k' = \log_2\left(1 + \frac{|\mathbf{h}_k^\mathsf{H}\mathbf{w}_k|^2}{|\mathbf{h}_k^\mathsf{H}\sum_{i\neq k}\mathbf{w}_i|^2 + \rho}\right), \tag{21}$$

where $\mathbf{W} = [\mathbf{w}_k, \ldots, \mathbf{w}_1, \ldots, \mathbf{w}_K]$ is the beamforming matrix satisfying $\|\mathbf{W}\|_F^2 \leq 1$ and $\mathbf{h}_k = [h_{1,k}, \ldots, h_{n,k}, \ldots, h_{N,k}]$. Here, the degrees of freedom are represented by the number of MISO array antenna elements and the HMISO Fourier modes, respectively, both indexed as n. The proposed HMISO system demonstrates superior performance compared to both MISO and Fourier-based HMISO configuration across the entire range of SNR values, surface lengths, and MISO array antenna spacings Δ. Indeed, the eigen-bases derived from the channel operator (11) and (12) are known to be the optimal communication modes when the noise is modeled as a spatially-uncorrelated Gaussian random field [5]. Notably, HMISO requires a number of RF chains equal to the number of transmitted modes only, namely $N = K$. Instead, the number of RF chains in the MISO and Fourier-HMISO systems increases proportionally with the surface length a as $\lfloor a/\Delta + 1 \rfloor^2$ and $\lfloor 4a^2/\lambda^2 \rfloor$, respectively. However, in the latter case, if one is able to select the modes with maximal intensity towards the receivers, the number of the needed RF chain can be reduced [3]. To achieve performance comparable to the eigen-based HMISO, the fully-digital MISO system must significantly reduce the antenna spacing, while the Fourier-based HMISO must operate at smaller wavelengths. In both cases, this leads to an increase in the number of RF chains, hence in the complexity of both manufacturing and power optimization.

Compared with these baselines, the proposed method introduces a higher complexity to obtain the bases due to the need of diagonalizing a rank-$3K$ matrix, as discussed in Section III-C. Nevertheless, it achieves substantial computational saving during signal processing. In fact, the optimization of the beamforming matrix in (21) involves NK complex coefficients, with $N \gg K$ the total number of Fourier modes or MISO array elements, while power optimization in (20) requires only K real coefficients.

V. Conclusion and Future Works

This work proposes a low-complexity eigen-based model for multi-user HMISO systems in continuous space. Using dipole-modeled receivers and an *ansatz* of weighted point-source fields, the channel is diagonalized with linear complexity in user count. A localized and orthogonal receiver basis is achieved via linear post-processing, and supports a 2:1 ratio of transmitting modes to users. The proposed method outperforms both Fourier-based HMISO and fully-digital MISO in spectral efficiency with fewer RF chains. Future work will extend the model to receivers with finite volumes by introducing coarse grids to sample the channel operator over each receiver. Further, discrete holographic architectures will be investigated to fill the gap with continuous surface modeling. Finally, more realistic wireless environments will be explored by incorporating hardware impairments and adapting the Green's function to model fading and ground reflections.

References

[1] T. Gong, P. Gavriilidis, R. Ji, C. Huang, G. C. Alexandropoulos, L. Wei, Z. Zhang, M. Debbah, H. V. Poor, and C. Yuen, "Holographic MIMO Communications: Theoretical Foundations, Enabling Technologies, and Future Directions," *IEEE Commun. Surv. Tut.*, vol. 26, no. 1, pp. 196–257, 2024.

[2] R. Deng, B. Di, H. Zhang, Y. Tan, and L. Song, "Reconfigurable Holographic Surface-Enabled Multi-User Wireless Communications: Amplitude-Controlled Holographic Beamforming," *IEEE Trans. Wireless Commun.*, vol. 21, no. 8, pp. 6003–6017, 2022.

[3] G. Iacovelli, C. Iacovelli, and S. Chatzinotas, "Holographic MIMO Surfaces: A Channel Model Approximation in the Electromagnetic Domain," *IEEE Wireless Commun. Lett.*, vol. 14, no. 2, pp. 305–309, 2025.

[4] M. Qian, L. You, X.-G. Xia, and X. Gao, "On the Spectral Efficiency of Multi-User Holographic MIMO Uplink Transmission," *IEEE Trans. Wireless Commun.*, vol. 23, no. 10, pp. 15 421–15 434, 2024.

[5] L. Sanguinetti, A. A. D'Amico, and M. Debbah, "Wavenumber-Division Multiplexing in Line-of-Sight Holographic MIMO Communications," *IEEE Trans. Wireless Commun.*, vol. 22, no. 4, pp. 2186–2201, 2023.

[6] D. A. B. Miller, "Communicating with waves between volumes: evaluating orthogonal spatial channels and limits on coupling strengths," *Appl. Opt.*, vol. 39, no. 11, pp. 1681–1699, Apr 2000.

[7] J. C. Ruiz-Sicilia, M. D. Renzo, M. D. Migliore, M. Debbah, and H. V. Poor, "On the Degrees of Freedom and Eigenfunctions of Line-of-Sight Holographic MIMO Communications," 2023. [Online]. Available: https://arxiv.org/abs/2308.08009

[8] Z. Wan, J. Zhu, Z. Zhang, L. Dai, and C.-B. Chae, "Mutual Information for Electromagnetic Information Theory Based on Random Fields," *IEEE Trans. Commun.*, vol. 71, no. 4, pp. 1982–1996, 2023.

[9] L. Wei, T. Gong, C. Huang, Z. Zhang, W. E. I. Sha, Z. N. Chen, L. Dai, M. Debbah, and C. Yuen, "Electromagnetic Information Theory for Holographic MIMO Communications," 2024. [Online]. Available: https://arxiv.org/abs/2405.10496

[10] Z. Wan, J. Zhu, and L. Dai, "Can Continuous Aperture MIMO Obtain More Mutual Information Than Discrete MIMO?" *IEEE Commun. Lett.*, vol. 27, no. 12, pp. 3185–3189, 2023.